

Content from this work may be used under the terms of the CC BY 3.0 licence (© 2019). Any distribution of this work must maintain attribution to the author(s), title of the work, publisher, and DOI

# RECONFIGURATION OF SPS LANDAU OCTUPOLE CIRCUITS TO MINIMISE SECOND ORDER CHROMATICITY

H. Bartosik\*, M. Carlà, K. Cornelis,  
 CERN, Geneva, Switzerland

## Abstract

In the SPS Q20 optics presently used for LHC beams, the Landau octupole families of the SPS (LOF and LOD circuits) generate large second order chromaticity due to the relatively high dispersion at their locations. Since the induced second order chromaticity results in enhanced losses due to the large incoherent tune spread, these octupoles cannot be used for mitigating transverse instabilities for LHC beams. A new cabling scheme was proposed, exploiting additional octupoles that were already installed in the machine but not used, which allows minimizing the induced second order chromaticity in both the Q20 optics used for LHC beams, as well as the original SPS optics used for fixed target beams. This paper summarises the optics calculations as well as the experimental verification of the reduced chromatic detuning of the new octupole scheme.

## INTRODUCTION

The Super Proton Synchrotron (SPS) at CERN delivers beam to the North Area fixed-target experiments as well as to the HiredMat and AWAKE facilities, and serves as injector for the Large Hadron Collider (LHC). Since the SPS transverse damper is not sufficient to fully suppress resistive wall instabilities of the high intensity fixed target beams, Landau octupoles are used in routine operation to generate amplitude dependent detuning and stabilise the beam. On the other hand, for LHC beams in the present operational intensity range (up to  $1.3 \times 10^{11}$  p/b) Landau octupoles are not required for routine operation as in this case the transverse damper is sufficient for suppressing coupled bunch instabilities. However, horizontal coupled bunch instabilities have been encountered for LHC beams with intensities above  $1.8 \times 10^{11}$  p/b during machine development studies even with the transverse damper [1]. For comparison, after the LHC injectors upgrade (LIU) project [2, 3], the SPS needs to deliver  $2.3 \times 10^{11}$  p/b to the LHC and thus mitigation measures for this horizontal instability have to be prepared. A possible solution would be to use the Landau octupoles also for the operation of the future LHC beams [1].

The SPS has one family of Landau octupoles at positions with large horizontal beta-function, called LOF circuit, and another family at positions with large vertical beta-function, called LOD circuit. Fixed target beams are operated with the original SPS optics configuration with integer tunes of 26 ("Q26" optics). Since 2012 a low transition energy optics with integer tunes of 20 ("Q20" optics) is used in routine operation for LHC beams to overcome single bunch vertical instabilities in preparation of the LIU upgrade [4–6].

\* hannes.bartosik@cern.ch

## OLD OCTUPOLE SCHEME

The Landau octupoles in their old configuration induced large  $Q''$  (second order chromaticity) in the Q20 optics. Figure 1 shows the measured horizontal and vertical tune shift as a function of momentum offset for normalised octupole settings of  $k_{LOF} = 2 \text{ m}^{-4}$  and  $k_{LOD} = 2 \text{ m}^{-4}$  in comparison to the optics model in the Q20 optics. The quadratic dependence due to the induced  $Q''$  is evident. The range of relative momentum deviations shown here correspond to the bucket height of LHC beams at SPS injection with operational RF voltage settings. It should be emphasised, that the amplitude detuning for these octupole settings is about one order of magnitude smaller considering particles 4 standard deviations away from the center of a beam with typical normalised transverse emittances of  $2 \mu\text{m}$  at the SPS injection plateau of 26 GeV/c.

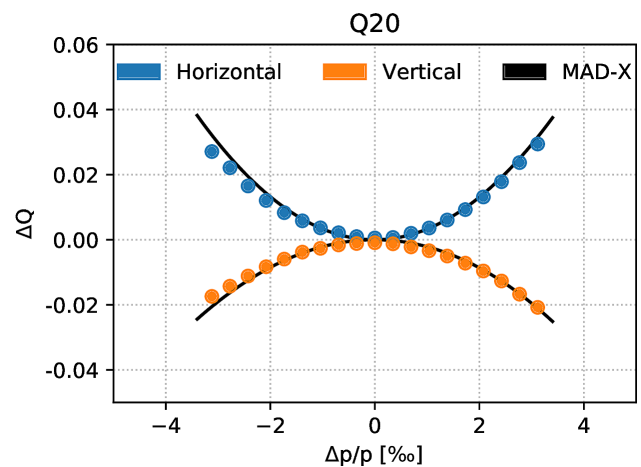


Figure 1: Measured tune shift as a function of momentum offset compared to the optics model prediction for octupole settings of  $k_{LOF} = 2 \text{ m}^{-4}$  and  $k_{LOD} = 2 \text{ m}^{-4}$ .

The induced  $Q''$  restricted the usable octupole strength for Landau damping of LHC beams: Figure 2 shows the measured accumulated losses at the end of the flat bottom and at the end of the cycle (i.e. including acceleration) for an LHC beam in the Q20 optics as a function of the normalised octupole strength of the LOF circuit. Within the range of  $-3 \text{ m}^{-4} \leq k_{LOF} \leq 5 \text{ m}^{-4}$  the flat bottom losses are slightly enhanced, but the total losses remain the same. In other words, the octupoles provoke flat bottom losses of particles, which would be lost during acceleration otherwise. When the octupole strength is increased beyond these limits, the total losses increase. This behaviour can be understood considering that the LHC beam injected into the SPS has large longitudinal tails resulting in full RF buckets and part

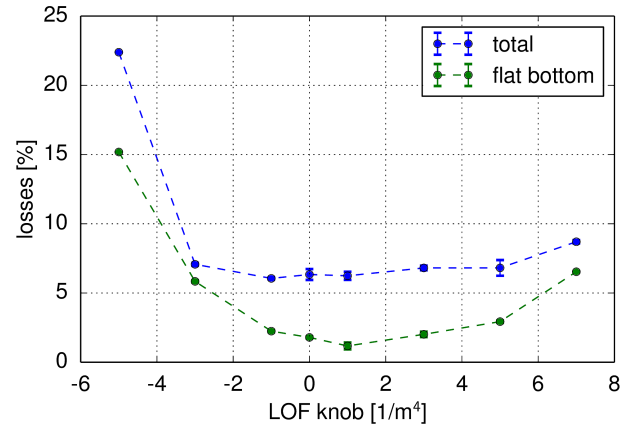


Figure 2: Losses on flat bottom (green) and total losses including acceleration (blue) as a function of octupole strength of the LOF circuit for an LHC beam in the Q20 optics.

of the beam not even captured by the SPS RF system [7]. Thus, there are particles with large momentum offset circulating in the SPS and the induced  $Q''$  can shift their tune onto resonances (e.g. integer and half-integer). In fact, for  $k_{LOF} \leq -5 \text{ m}^{-4}$  the induced  $Q''$  is so large that even particles within the RF bucket reach the horizontal integer resonance.

The contribution of octupoles to second order chromaticity can be calculated as

$$Q''_{x,y} = \pm \frac{1}{2 \times 4\pi} \oint \beta_{x,y}(s) K_3(s) D_x^2(s) ds, \quad (1)$$

where  $\beta_{x,y}(s)$  are the optical beta functions,  $K_3(s)$  is the normalised octupole strength and  $D_x(s)$  is the horizontal dispersion function. Figure 3 shows a schematic of the old

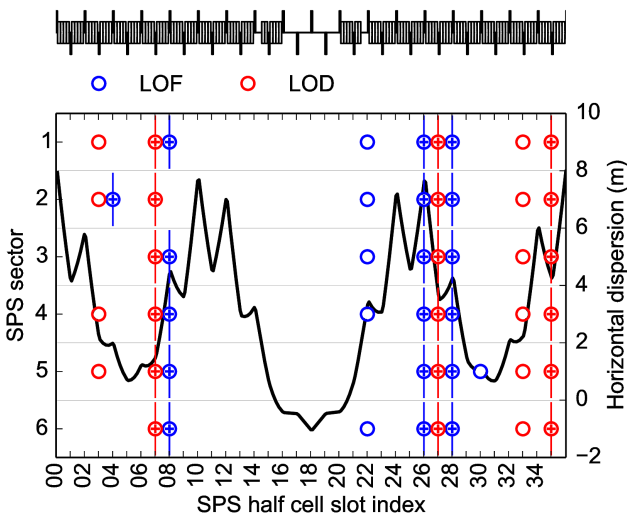


Figure 3: Schematic of the old SPS octupole scheme. The location of octupoles in the lattice is indicated by markers for LOF (blue) and LOD (red) octupoles for each sextant, where the symbol inside the marker indicates the polarity (“+” for normal, empty markers for disconnected). The dispersion function of the Q20 optics is also shown.

octupole scheme of the SPS together with the dispersion function in the Q20 optics. Note that the dispersion function performs resonant oscillations in the arcs since the phase advance per arc is about  $3 \times 2\pi$  [4]. Therefore the dispersion function reaches relatively large peak values. In particular, the dispersion is quite large at the locations of the octupoles (at least of some of them). This explains the large  $Q''$  generated by the octupoles in the Q20 optics. In the Q26 optics on the other hand the induced  $Q''$  is much smaller because the dispersion function evolves differently along the arcs (phase advance of  $4 \times 2\pi$  per arc) and its value is much smaller at the location of the octupoles. The arrangement of octupoles follows in general the six-fold symmetry of the SPS lattice (except for two LOF octupoles that had to be moved in the past to make space for special equipment, and two missing LOD octupoles). However, not all of the Landau octupoles installed in the SPS were actually powered in the old scheme, but some were simply disconnected.

## OCTUPOLE RECONFIGURATION

The SPS octupole scheme was reconfigured in September 2018 during a technical stop with the aim of minimizing the octupole induced  $Q''$ . Figure 4 shows a schematic of the new octupole scheme. Note that the polarity of the octupoles at locations with the maximum dispersion in the Q20 optics have been inverted in both the LOF and the LOD circuit. This allows best cancellation of the overall contribution to  $Q''$  from all octupoles, as their individual contribution is proportional to the square of the local dispersion function (Eq. 1). However in this case the contribution to amplitude detuning is also partially cancelled due to the polarity inversion. Therefore additional octupoles (already installed in the

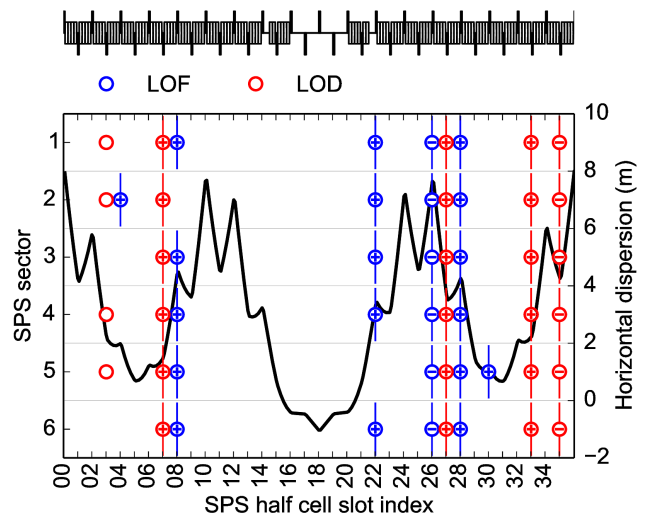


Figure 4: Schematic of the new SPS octupole scheme. The location of octupoles in the lattice is indicated by markers for LOF (blue) and LOD (red) octupoles for each sextant, where the symbol inside the marker indicates the polarity (“+” for normal, “-” for reversed, empty markers for disconnected). The dispersion function of the Q20 optics is also shown.

Content from this work may be used under the terms of the CC BY 3.0 licence (© 2019). Any distribution of this work must maintain attribution to the author(s), title of the work, publisher, and DOI

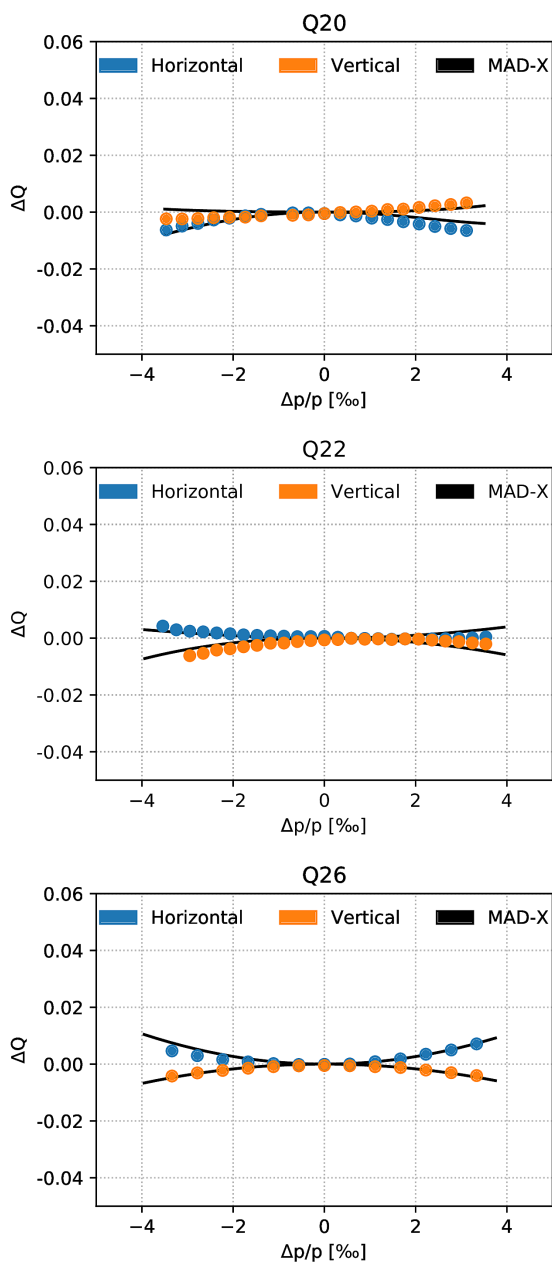


Figure 5: Measured tune shift as a function of momentum offset compared to the optics model prediction for octupole settings of  $k_{LOF} = 3 \text{ m}^{-4}$  and  $k_{LOD} = 3 \text{ m}^{-4}$  for the Q20 optics (top), the Q22 optics [8] (middle) and the Q26 optics (bottom).

machine but previously disconnected) have been included in the circuits. In the new configuration, two octupoles per sextant effectively generate amplitude detuning compared to three octupoles in the old configuration. This means that, in the new configuration, 1.5 times higher octupole strength is needed to achieve the same amplitude detuning. Figure 5 shows the measured horizontal and vertical tune shift as a function of momentum offset with the new octupole scheme for normalised octupole settings of  $k_{LOF} = 3 \text{ m}^{-4}$  and  $k_{LOD} = 3 \text{ m}^{-4}$  in comparison to the optics model for the available SPS optics configurations. It should be emphasized that

Table 1: Comparison of SPS Octupole Schemes

LOF position	08/04	22/30	26	28	
Old polarity	+	0	+	+	
New polarity	+	+	-	+	
LOD position	03	07	27	33	35
Old polarity	0	+	+	0	+
New polarity	0	+	+	+	-

these settings produce the same amplitude detuning as for the measurement in the old scheme shown in Fig. 1. The clear reduction of the induced  $Q''$  is observed. Furthermore it should be pointed out that similarly low values of  $Q''$  are achieved in all presently available SPS optics configurations.

A comparison of the octupole polarities between the old and the new scheme is summarised in Table 1 for the various octupole positions in the SPS lattice (in half cell slots), where “+” means normal polarity, “-” means inversed polarity and “0” means disconnected. It should be emphasised that the modification of the octupole circuits could be achieved by an intervention on the patch panels of the corresponding magnets and thus did not require major hardware modifications. The power converters for the SPS Landau octupole circuits provide largely sufficient margin for the operationally required octupole currents in this new configuration even considering that 1.5 times higher octupole strength is needed for the same amplitude detuning (operational values of up to 50 A were used for fixed target beams in the old configuration, while the maximum available current is more than 200 A). However, the power converters had to be retuned for the increased load and this resulted in a reduced achievable rate of current change  $dI/dt$ . This required a change in the cycling of the magnets at the end of each SPS cycle (when the beam is already extracted), but there is no issue for programming of the octupole functions during beam presence (as only slow variations during acceleration are needed).

## CONCLUSION

In their original configuration the SPS Landau octupoles could not be used for curing transverse instabilities for LHC beams, as they induced large  $Q''$  which limited the usable octupole strength due to incoherent losses. After the re-configuration of the octupole circuits, the induced  $Q''$  is significantly reduced as expected from optics simulations and confirmed in measurements, and is now similar in all available SPS optics. This opens the possibility of using the Landau octupoles also for the stabilization of transverse instabilities with LHC beams, as already exploited in machine development studies at the end of 2018 [1].

## ACKNOWLEDGEMENTS

The authors would like to thank J. Bauche and his team for performing the cabling modifications on the SPS octupole circuits, and J. Le Godec and his team for the retuning of the power converters to the new load.

## REFERENCES

- [1] M. Carlà *et al.*, “Transverse beam dynamics studies with high intensity LHC beams in the SPS”, in *Proc. 10th Int. Particle Accelerator Conf. (IPAC'19)*, Melbourne, Australia, May 2019, paper MOPTS089, this conference.
- [2] J. Coupard *et al.*, “LHC Injectors Upgrade, Technical Design Report, Vol. I: Protons”, LIU Technical Design Report (TDR), CERN-ACC-2014-0337.
- [3] M. Meddahi *et al.*, “LHC Injectors Upgrade Project: Towards New Territory Beam Parameters”, in *Proc. 10th Int. Particle Accelerator Conf. (IPAC'19)*, Melbourne, Australia, May 2019, paper THXPLM1, this conference.
- [4] H. Bartosik, G. Arduini, and Y. Papaphilippou, “Optics Considerations for Lowering Transition Energy in the SPS”, in *Proc. 2nd Int. Particle Accelerator Conf. (IPAC'11)*, San Sebastian, Spain, Sep. 2011, paper MOPS012, pp. 619–621.
- [5] H. Bartosik, G. Iadarola, Y. Papaphilippou, G. Rumolo, B. Salvant, and C. Zannini, “TMCI Thresholds for LHC Single Bunches in the CERN-SPS and Comparison with Simulations”, in *Proc. 5th Int. Particle Accelerator Conf. (IPAC'14)*, Dresden, Germany, Jun. 2014, pp. 1407–1409. doi:10.18429/JACoW-IPAC2014-TUPME026
- [6] Y. Papaphilippou *et al.*, “Operational Performance of the LHC Proton Beams with the SPS Low Transition Energy Optics”, in *Proc. 4th Int. Particle Accelerator Conf. (IPAC'13)*, Shanghai, China, May 2013, paper THPWO080, pp. 3945–3947.
- [7] H. Timko *et al.*, “Longitudinal transfer of rotated bunches in the CERN injectors”, *Phys. Rev. ST Accel. Beams*, 16, 5, 051004, 10.1103/PhysRevSTAB.16.051004, 2013.
- [8] M. Carlà, H. Bartosik, M. S. Beck, K. S. B. Li, and M. Schenk, “Studies of a New Optics With Intermediate Transition Energy as Alternative for High Intensity LHC Beams in the CERN SPS”, in *Proc. 9th Int. Particle Accelerator Conf. (IPAC'18)*, Vancouver, Canada, Apr.-May 2018, pp. 713–716. doi:10.18429/JACoW-IPAC2018-TUPAF022